IEEE Access
Multidisciplinary | Rapid Review | Open Access Journal

Received 17 May 2023, accepted 29 June 2023, date of publication 11 July 2023, date of current version 20 July 2023.

Digital Object Identifier 10.1109/ACCESS.2023.3294275

APPLIED RESEARCH

DNN-Based Prediction of Standard Driving Posture for Vehicle Takeover

JUNJIE GOU, (Member, IEEE), MINGMING ZHAO, HONGYAN WANG, AND XIAN WU
School of Automotive Studies, Tongji University, Shanghai 200092, China
Corresponding author: Xian Wu (wuxian@tongji.edu.cn)

ABSTRACT When drivers need to take over a vehicle during shared autonomy, the standard driving postures based on their body size are the basis of non-driving posture (NDP) motion reconstruction. This study focused on the prediction of standard driving postures using a deep learning neural network (DNN) method. Firstly, the main factors influencing the standard driving posture were extracted through qualitative analysis, and their weights were analyzed using an orthogonal test method. Based on this, the main parameters of the standard driving posture prediction model were determined. Secondly, the point cloud data of typical vehicles on the market were obtained through laser scanning. After extracting the key input and output parameters required for the prediction model through point cloud data processing and feature matching, a dataset of standard driving postures was established. Finally, a supervised learning model using a deep learning neural network (DNN) was established to predict the standard driving postures of different drivers under different vehicle package layouts. This method allows for the quick evaluation of corresponding standard driving postures during non-driving activities, laying the foundation for risk-level assessment of non-driving postures and motion reconstruction in vehicle takeover. The results show that the trained algorithm model can predict standard driving postures with high accuracy and robustness.

INDEX TERMS Driving posture prediction, NDP, DNN, vehicle takeover.

I. INTRODUCTION

Due to the limitations of the current autonomous driving technology's development, human beings would be in the model of shared autonomy for a long time in the future. Increasing numbers of drivers admit to using smartphones while driving and engaging in increasingly complex and dangerous activities such as texting, taking photos, browsing the internet, and using social networks. These non-driving tasks cause their hands, feet, eyes, and minds to move further away from the primary driving task in increasingly complex and hazardous ways, resulting in physical, sensory, and cognitive distractions [1], [2], [3], [4]. Non-driving activities (NDRT) would result in an increasing number of non-standard driving postures, which pose new challenges to traditional passive safety protection and seriously threaten driving safety [5], [6], [7]. When confronted with abrupt and hazardous circumstances that the system is incapable of handling, the successful takeover process within a specific timeframe necessitates the driver's cognitive, sensory, and motor reconfiguration. To accurately reconstruct the non-standard driving posture, it is imperative to acquire the current driver's optimal takeover state, also known as the standard driving posture, and measure the deviation between the current non-standard driving posture and the standard driving posture. As such, precise prediction of the current driver's standard driving posture is paramount for reconstructing non-standard driving postures(NDPs) and evaluating takeover ability.

The standard driving posture is the initial state of the current driver which meets the requirements of safety and comfort design. In the design of standard driving posture, SAE has provided a reference line for the H-point, which is used to determine the location of the H-point (the hip point) for different percentile human models [8]. However, this reference line is known to deviate from the actual driving posture in China, of the huge difference in human body size between China and the United States. Park et al. found that there are significant differences in body size and proportions

The associate editor coordinating the review of this manuscript and approving it for publication was Mitra Mirhassani.

between Europeans and Asians, resulting in markedly different driving postures [9]. Mehta and Tewari proposed a design model for seats and postures based on biomechanics, which includes medical, human factors engineering, psychology, and physiology [10], but the size of the dataset is limited and mainly to study the driving uncomfortable which can't support the quick response of driving takeover. Chai Chunlei studied the factors influencing driving posture in his doctoral dissertation through experimental research, including body size, steering wheel, pedals, etc. The quantitative relationship between some influencing factors and driving posture was studied using statistical methods, and a prediction model for driving posture was established [11]. However, the weight of the influencing factors has not been fully investigated, which means the quantitative analysis is not enough, while the motion reconstruction needs a detailed quantitative analysis of standard driving posture.

In addition, some researchers have used machine learning methods for driving posture prediction, such as linear regression prediction [12], support vector machine theory [13], fuzzy theory [14], and neural networks [15]. However, due to the quality and the sample size of the data set, the accuracy of the prediction models still have some shortcomings, and its model construction does not fully consider the influence of factors such as the diversity of people and the different arrangements of vehicles. Relatively speaking, neural networks fit better in dealing with complex datasets with multiple input parameters. Among them, DNN has a better fitting ability than BP neural network model and can accomplish the same task with fewer data and use the data effectively.

In summary, a quick prediction of the current driver's standard driving posture forms the benchmark for reconstructing the NDP. Current prediction methods are not adequate for fast and personalized prediction of standard driving postures, and new prediction methods need to be constructed. Considering the actual demand for a supervised prediction model in this paper, the DNN neural network was selected.

Besides, this paper focuses on the kinematic reconstruction of the standard driving posture, therefore, the influence of the driver's psychology and driving behavior habits on the standard driving posture is not within the scope of this article.

The contribution of this paper can be summarized as follows:

1) Little research has been done on motion reconstruction in vehicle takeover because it is difficult to personally quantify the amount of motion reconstruction for individuals, which is the difference between the current driving stance and its corresponding standard driving stance, and translate it into the amount of motion of the driving components. In this paper, we provide a DNN-based prediction method for personalized standard driving posture considering human diversity, which offers the possibility of motion reconstruction for NDP and can be used as a benchmark for current driver's motion reconstruction.
2) Compared with other simulation analysis methods, the prediction method in this paper can achieve real-time prediction of standard driving posture, thus supporting the motion reconstruction of NDP to meet the application requirements.
3) A dataset containing multimodal truth value is constructed for model training of standard driving postures. Using laser scanning and model simulation technology, the vehicle, and ergonomic parameters of more than 43 cars were collected, and the high weights influence factors of the standard driving posture design were fully considered. This dataset has important applications as a study of the standard driving posture of drivers.
4) The weights of each influencing factor of the standard driving posture were analyzed, and the data-driven forward design of the standard driving posture was constructed based on DNN.

II. STANDARD DRIVING POSTURE DESIGN

In this section, the main influence parameters of standard driving posture were extracted through qualitative analysis, the weights of important parameters were analyzed by the orthogonal test method, and the prediction model of standard driving posture could be constructed considering the convenience of parameters measurement and their influence weights. In my previous study, a detailed analysis was presented, we highlight the significant influence of diverse human body dimensions on the design of the standard driving posture and provide corresponding corrective measurements [16].

A. FACTORS CONSIDERATION OF POSTURE DESIGN

The standard driving posture design of a vehicle is related to many factors [17], like the vehicle size, manikin size, steering wheel position, pedal position, seat backrest angle, vision ability, and room ability, etc.

The first part is the vehicle's target user. Drivers from areas around the world have different body sizes, which in turn require different driving postures. Many vehicles designed by foreign companies have complained in China about their driving posture, such as Mercedes-Benz GLA, which has poor headroom performance. So, the dummy size would be a considered reason.

The second part is the dimension of the vehicles. Different sizes and types of vehicles would have a huge impact on the driving posture design. The length would influence the X position of the driver inside the vehicle and the dimension of L99, the distance of X-direction between the SgRP(seat reference point) and BOF(ball of the foot), which is the key point for the package of pedal and seat. The width would change the driver's side room ability. Besides, height is the most important part of posture design, for the different heights would result in little choice of seat height(H30), which is the first confirm size of posture design.

The third part is the package layout of the vehicle and ergonomics demand. To start with, for the driver's posture, the package of the steering wheel is an important consideration, which determines the driver's leg room and chest impact room. Thus, we select the size of the distance between the steering wheel and the AHP (heel point) as the important factor. Secondly, the convenience of the driver's entry and exit would be affected greatly by the rocker, which is related accordingly to the height of the driver's seat. In this experiment, the height of the rocker (H130-1) could be chosen as an important factor.

Furthermore, the driver's vision would prompt the driver to adjust the seat height, and in turn, impact the headroom. As we all know, many female drivers like to sit highly to obtain a better vision of the forward road, and the driver would have a sense of local crowding and depression, if headroom is not enough. Based on them, we select the front under vision(A124-1-L) and headroom (H61-1) as the important influence factors.

Finally, other factors, such as the grasping position of the steering wheel and the arm length, also influence the design of the standard driving posture, but considering the settings and limitations of the simulation software, the grasping position could be definite to the symmetrical position and the arm length could be automatically changed together with the body height.

B. FACTORS INFLUENCE WEIGHTS

The driving posture is simulated by constructing the human model and the elements of the vehicle ergonomics based on the software of RAMSIS. The weights of the influencing factors of standard driving posture are measured by an orthogonal experiment. The environmental data of the simulation analysis is shown in Figure 1.

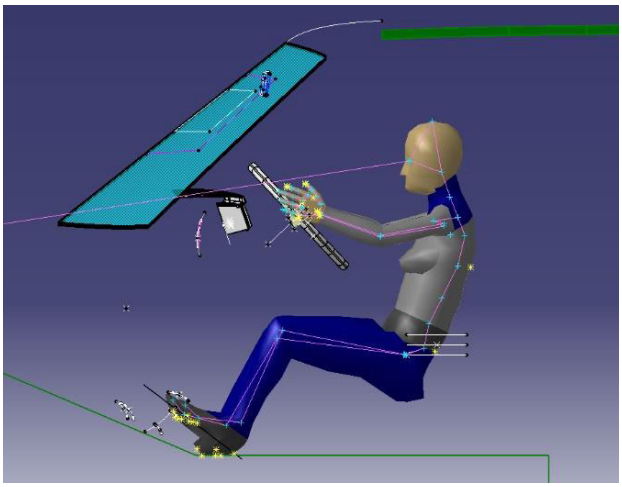

FIGURE 1. Simulation data of RAMSIS.

Considering the setting requirements of RAMSIS, seven key influence factors are selected respectively, such as human body size, vision-forward down, the adjustment range of the steering wheel, A40, H30, and L99. After 18 groups of tests using the orthogonal test method, the weight coefficient R can be sorted in the order: L99 (R = 3.72), human model (R = 1.92), steering wheel height adjustment (R = 1.17), vision-forward down (R = 0.85), steering wheel axial adjustment (R = 0.68), H30 (R = 0.6), seat back angle A40 (R = 0.23), as shown in figure 2.

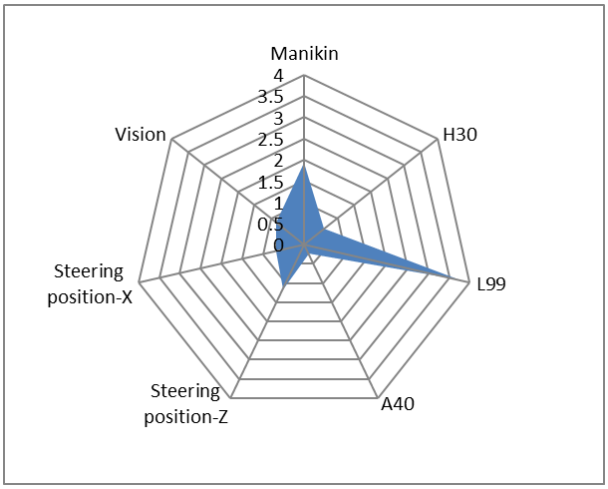

FIGURE 2. Factors influence weights.

Through the weight analysis, we make the following considerations in the parameter selection of the standard driving posture prediction model.

1) The influence weights of L99 and human body size are the highest, and the L99 is related to the 95th quartile male's thigh length and the X-direction dimension of the vehicle. Here, we use the manikin height and wheelbase(L101) as prediction model inputs.
2) The position of the steering wheel has a great influence on the standard driving posture. considering the difference between the convenience of actual measurement and the software simulation, we select the size distance between the steering wheel and the foot (L11/H17) as the inputs.
3) The forward-down vision is a key factor, so the vision-forward down(A124-1) can be chosen as the input.
4) H30 and L99 reflect the room ability of the vehicle, have a great influence on the design of the standard driving posture, and are closely related to the height of the vehicle and seat from the ground in the forward design. Based on the above information, we select the headroom (H61-1), the height of the rocker (H130-1), and the height of the vehicle(H101) as the inputs. The width of the vehicle could change the driver's side room ability, we use the size of width(W103) as input.
5) The influence weight of the A40 is low in the design of the standard driving posture, so it always can be set using a default value in the forward design (such as 25 degrees).

C. FACTORS SELECTION OF THE PREDICTION MODEL

The diver's posture is commonly characterized using three dimensions, H30, W20, and L53 [18], [19], [20], [21]. Among them, the distance of Z-direction between the driver's seat reference point (SgRP) and the heel point (AHP) is signed as H30. The distance of X-direction between the SgRP and AHP is characterized as L53. The distance of the Y-direction between SgRP and the longitudinal symmetry plane (Y0 plane) of the vehicle is signed as W20. These three dimensions are defined as the three output parameters of the model, which are denoted as Rx, Rz, and W20-1, as shown in FIGURE 3.

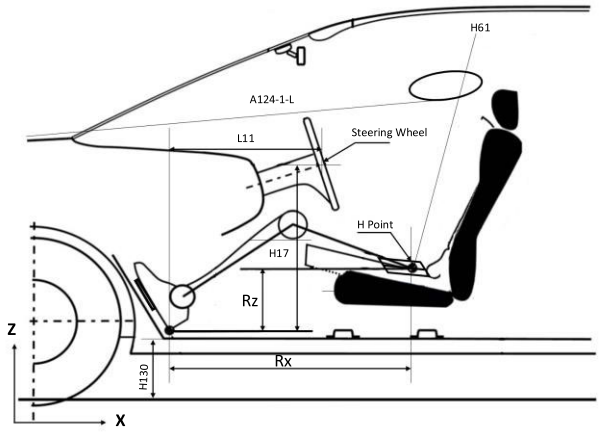

FIGURE 3. Factors selection of the prediction model.

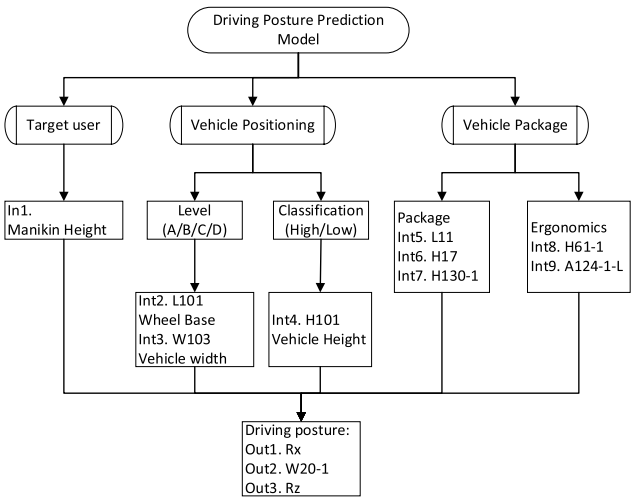

FIGURE 4. Prediction model of standard driving posture.

As we defined, the input and output parameters of the predicted model can be determined as follows. The input layer contains 9 parameters: Manikin height, W103, L101, H101, H103-1, H17, L11, H61-1, and A124-1-L. The output layer contains 3 parameters: Rx, W20-1, and Rz. The relationship between the model's input and output is shown in FIGURE 4.

III. STANDARD DRIVING POSTURE DATA SET

In this section, we collect the point cloud of the most popular vehicles using laser scanning. The key points of the vehicles can be extracted through processing and feature reconstruction.

The driving posture data set was constructed based on the selection of model factors, which take into the physical factors related to the human body, the position of the steering wheel, the driver's room ability, and so on. Besides, we believed that humans even don't know which posture is the most standard one, so human's subjective behavior is not the scope of this article.

A. VEHICLE INFORMATION OF THE EXPERIMENTS

Currently, vehicles sold in the market of China are from all over the world. Based on the height of the vehicles, they can be categorized as different types from A00-level to D-level referring to the general vehicle classification of Germany. According to our statistics, the typical cars on the current market, from A0 to D, were selected for the experiments. Specifically, there are 3 A0-class sedans, 9 A-class sedans, 2 B-class sedans, 16 A-class SUVs, 2 C-class sedans, 10 C-class SUVs, and 1 D-class sedan. The detailed information about vehicles in our tests is shown in Table 1.

TABLE 1. Typical vehicles of China.

No.	Car	Class	No.	Car	Class
1	FIAT500	A0	23	CS35	ASUV
2	IQ	A0	24	CS75	ASUV
3	MIEV	A0	25	KUGA	ASUV
4	BAOJUN630	A	26	RUIHU 5	ASUV
5	FOCUS	A	27	KIA ZHIPAP	ASUV
6	GOLF	A	28	TIGUAN	ASUV
7	JEETA	A	29	IX35	ASUV
8	BORA	A	30	QASHQAI	ASUV
9	SAIL	A	31	A6	C
10	C30	A	32	ROEV950	C
11	C50	A	33	Q7	CSUV
12	AVANZA	A	34	BMW X5	CSUV
13	A5	B	35	CAYENNE	CSUV
14	K5	B	36	RANGE	CSUV
15	CRV	ASUV	37	VX	CSUV
16	RAV4	ASUV	38	PAJERO	CSUV
17	Q3	ASUV	39	GRAND	CSUV
18	BMW X1	ASUV	40	TOUAREG	CSUV
19	FORD ECO	ASUV	41	RAN-USA	CSUV
20	HAVL H6	ASUV	42	XC90	CSUV
21	HAVL M4	ASUV	43	A8	D
22	S3	ASUV			

It is worth pointing out that due to China's huge vehicle market, we cannot collect all the hot-selling vehicle' data. However, the 43 vehicle models selected above have contained typical cars of different types, which are sufficient to support our research work. After the vehicle models

were determined, point cloud technology is involved to obtain the hard points related to the driving posture prediction.

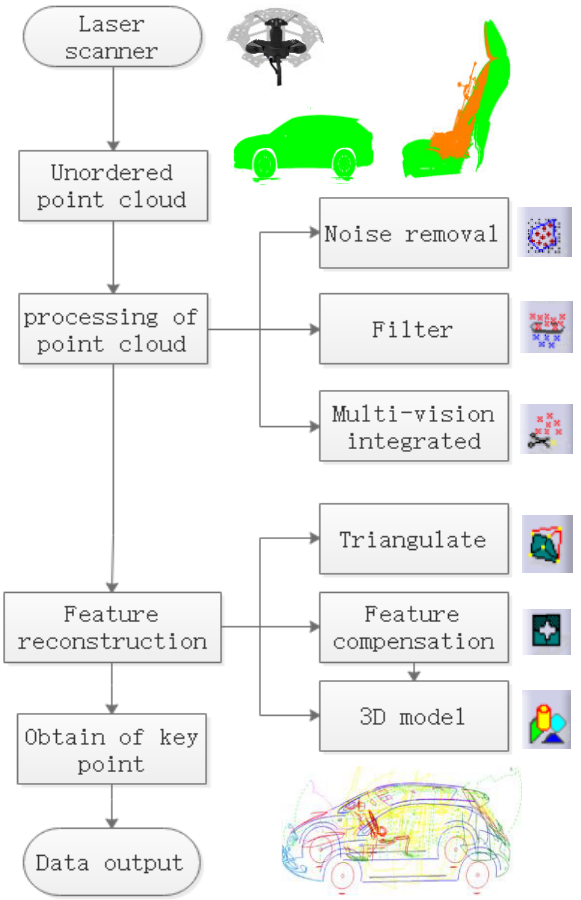

FIGURE 5. Flow chart of point cloud data processing.

B. PROCESSING FLOW OF POINT CLOUD

The point cloud data from the previous work were used for this study. The total data set size exceeds 285.2G. We can see the overview of the point cloud processing flow in FIGURE 5. Here, we just briefly review the point cloud data processing flow, the details can be seen from my previous work [22].

Compared with traditional scanning methods, laser scanning can quickly obtain three-dimensional dense point clouds of the vehicle. The target vehicle's point cloud big data is collected by equipment from a Canadian company named CREAFORM. The laser scanning equipment can be divided into three parts: the hand-held scanning probe, the controller, and the receiver. Through the link of the data line between the hand-held scanning probe and the receiver, the demand data of the point cloud can be obtained by using the specific built-in software. Using laser scanning, the big data of the point cloud can be obtained in terms of the contour of the target vehicle and driver's seat in different extreme states. Thus, the vehicle dimensions for driving posture prediction can be obtained, such as length, width, height, wheelbase, the coordinates of the H point, and so on.

Normally, the initial point cloud obtained is disordered, the preprocessing would go through three steps which are noise removal, data filtering, cleaning, and feature reconstruction to extract the valuable data hidden in the initial database [23].

Firstly, the noise of the point should be removed, otherwise, the data processing will be greatly interfered with by the mixed noise [24]. We need to remove the redundant and non-characteristic information as soon as possible. Secondly, the data of the point cloud should be filtered and cleaned on the premise of satisfying the feature extraction, to reduce the subsequent calculation [25]. Finally, the acquired point cloud data is integrated and aligned based on typical feature alignment and other methods. It is necessary to adjust multiple point cloud data to appropriate coordinates [26], [27], which conform to the normal observation angle.

After the point cloud data cleaning, the feature reconstruction would be conducted. We use the software of CATIA to build the three-dimensional (3D) key point models of the vehicles [28], [29]. Using the triangle grid get the information related to driving posture, and the missing holes and features are filled in, the boundary effect is optimized, and the corresponding curved surfaces and lines needed are fit. The hard point of the vehicle can be obtained, and the key points can be accessed quickly by feature reconstruction and stored in a more lightweight and visualized form.

C. DATA SET

Each curve represents the seat position of a typical human body. The group curve can represent the seat position of all human bodies [21]. In the engineering practice of automobile design, this curve is often used to determine the H-point area of the seat in the design stage, as shown in FIGURE 6.

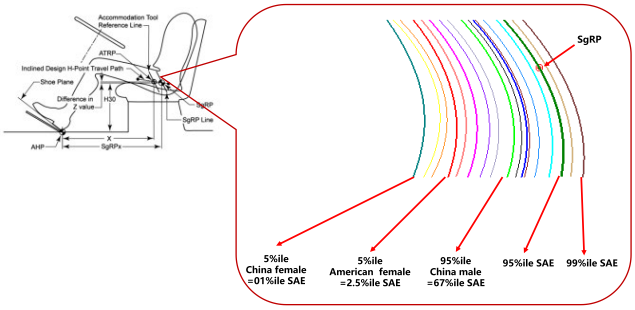

FIGURE 6. Reference line of H point.

Based on this curve, the scope of use range is expanded, it is range from P5 female of China to P99 SAE male. We can select the seat travel box of the hot-selling cars based on the SAE seat position reference curve and take the intersection of the midline of the stroke and the SAE seat reference curve. Each intersection represents a driving position corresponding to human size. The distances of X and Z directions between the intersection and the heel point are the required

TABLE 2. Training data for the neural network.

Option /No.	Input									Output		
	Int1	Int2	Int3	Int4	Int5	Int6	Int7	Int8	Int9	Ou1	Out2	Out3
	Manikin Height	L101	W103	H100	L11	H17	H130-1	H61-1	A124-1-L	Rx	W20-1	Rz
	mm	mm	mm	mm	mm	mm	mm	mm	degree	mm	mm	mm
1	1455	2300	1622	1582	297	670	321	987	7.4	611.7	-329.7	318.9
2	1462	2383	1728	1574	321	679	408	999	5.0	615.5	-330.1	349.0
3	1568	2550	1474	1677	318	674	355	1018	9.0	656.0	-299.0	337.7
4	1862	2595	1743	1482	376	638	375	991	5.4	802.0	-360.0	280.0
5	1484	2465	1690	1463	385	696	341	959	6.0	641.5	-335.0	321.2
6	1898	2500	1694	1488	441	642	373	1012	6.2	846.0	-333.5	264.0
7	1715	2300	1622	1582	297	669.5	321	986	7.4	736	-329.7	313
8	1825	2383	1728	1573.7	321	678.8	408	998.7	5	771.3	-330.1	336.7
9	1605	2550	1807	1670	344	665	407	996	6.8	663.4	-355.0	348.2
10	1642	2632	1799	1428	390	646	347	964	5.1	728.7	-352.4	267.6
11	1916	2600	1736	1442	455	631	379	999	5.1	870	-355	252
...	...	...	...	...	...	...	...	...	...	...	...	...

output parameters. Based on this method, 15 sets of parameters can be obtained in the above pattern example.

After the definition of factors, we can construct the data set of standard driving posture, which can support the work of the next step, as shown in Table 2.

IV. DNN-BASED PREDICTION OF DRIVING POSTURE

This section will introduce the use of DNN to predict standard driving posture and give a detailed design of the DNN model structure [30], [31], [32].

A. DEEP NEURAL NETWROK

The DNN model was divided into an input layer, two hidden layers, and an output layer. After the model training, it can be convenient to confirm the corresponding RgRP based on the initial given conditions, which is the predicted driving posture. As shown in FIGURE 7.

We use nine parameters like human body size, vehicle wheelbase, vehicle width, vehicle height, L11, H17, driver headspace, A124-1-L, and H130-1 as the input of the DNN network, and denote them with $X = \{x_1, x_2, \ldots, x_9\}$. At the same time, we use Rx, W20-1, and Rz as the model output, and denote them with $Y = \{y_1, y_2, y_3\}$.

In addition, in order to ensure that the DNN network has a good performance, we expand the number of neurons in each hidden layer to $M = 50$ Therefore, we can express the DNN model as a mapping function from the input layer to the output layer, which is expressed as follows:

$$\hat{Y}(k) = f(X(k)) \tag{1}$$

where k is the number of training iterations, and $\hat{Y}(k)$ represents the actual output of the DNN. Using $e_m(k)$ to represent

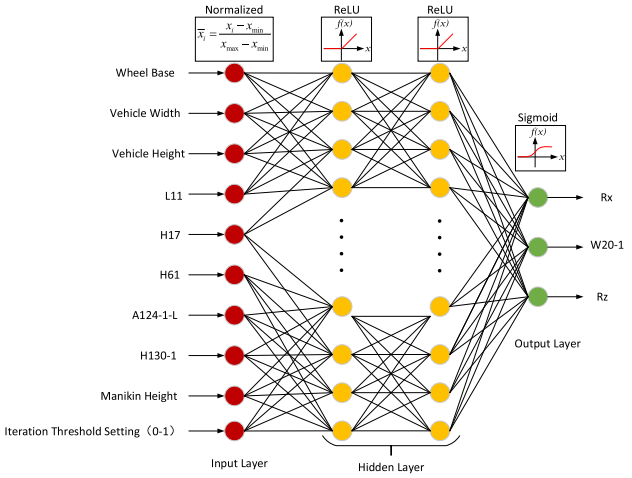

FIGURE 7. The designed DNN of the driving posture prediction model.

the signal error of the $m-th$ iteration of the $k-th$ neuron in the output layer, we have:

$$e_m(k) = Y(k) - \hat{Y}(k) \tag{2}$$

Therefore, the error energy of the DNN can be defined as:

$$e(k) = \frac{1}{2}\left(\sum_{m=1}^{M} e_m^2(k)\right) \tag{3}$$

Since our inputs are distributed in a wide range and have different physical meanings, it would be easy to cause some small or different dimension physical inputs to be obliterated in the DNN. To solve this problem, we would normalize all

inputs and outputs, the normalization rules are as follows:

$$\bar{x}_n = \frac{x_n - x_{min}}{x_{max} - x_{min}} \tag{4}$$

The $n-th$ sample value is x_n. The maximum and minimum values of the input layer are $x_{\max}$ and x_{min}, respectively. In addition, in order to prevent the hidden layer and the output layer from saturating the output of the neuron that is caused by the excessively large absolute value of the neurons' input, which will lead to the weight adjustment falling into the flat area of the error surface, we would check the hidden layer and the output layer's input of the neuron. In detail, we use the ReLU function to process the input of the hidden layer neurons, and the Sigmoid function to process the input of the output layer neurons. Thus, we can express the output of the $j-th$ neuron of the $i-th$ hidden layer as:

$$u_{i,j} = f\left(\sum\nolimits_l w^i_{j,l} u_{i-1,l} + e^i_j\right) \tag{5}$$

where $w^i_{j,l}$ represents the weight from the $l-th$ neuron of the $i-1-th$ hidden layer to the $j-th$ neuron of the $i-th$ hidden layer, and e^i_j represents the output error of the $j-th$ neuron of the $i-th$ hidden layer.

B. MODEL TRAINING

During the DNN model training process, the directional propagation algorithm was used to modify the weights, and the random gradient method adjusted the weights in batches to improve the training speed. The momentum method was introduced to modify the weight, for the gradient method would make the DNN model fall into the local minimum. in our training process. The weight correction scheme of the $j-th$ neuron in the $i-th$ layer to the $l-th$ neuron in the $i-1-th$ layer is as follows:

$$\Delta w^i_{j,l}(k) = \eta \sum\nolimits_s \delta^{i-1}_s x^{i-1}_s + \alpha \Delta w^i_{j,l}(k-1) \tag{6}$$

where η is the learning rate, δ^{i-1}_s is the local gradient on the $s-th$ neuron of the $i-1-th$ layer, x^{i-1}_s is the output of the $s-th$ neuron of the $i-1-th$ layer, and α is the momentum factor. In the above parameters, the momentum factor α generally takes the value between 0 and 1. The learning rate η and the value of the local gradient δ^{i-1}_s will be discussed next.

In the momentum gradient method, the learning rate is generally used to accelerate the convergence of the algorithm. By adjusting the learning rate, a relatively larger gradient far from the optimal point can be achieved, thereby reducing the number of iterations. On the contrary, by adjusting the learning rate, the momentum method will ensure convergence with a smaller gradient in the optimal point. To prevent the algorithm from oscillating, in our algorithm, we use iterative error to adjust the learning rate. When the error energy of the DNN decreases, it means that our algorithm is converging in the correct direction. Currently, we need to reduce the gradient, otherwise, we need to increase the gradient. The specific adjustment scheme is as follows:

$$\eta(k+1) = \begin{cases} \min\left\{\exp\left[\frac{\mathrm{e_{max}} - \mathrm{e}(k+1)}{\mathrm{e_{max}} - \mathrm{e_{min}}}\right], \theta_{\mathrm{up}}\right\} \\ \eta(k), \mathrm{e}(k+1) < \mathrm{e}(k), \\ \max\left\{\frac{\mathrm{e}(k+1) - \mathrm{e_{min}}}{\mathrm{e_{max}} - \mathrm{e_{min}}}, \theta_{\mathrm{low}}\right\} \\ \eta(k), \mathrm{e}(k+1) > \mathrm{e}(k), \end{cases} \tag{7}$$

Among them, θ_{up} and θ_{low} are the up-increment factors and the down-increment factor, respectively, usually we have, $\theta_{up} \in [1.2, 10]$ and $\theta_{low} \in [0.2, 0.8]$

The local gradient characterizes the changing trend of the weights of a certain neuron and its adjacent layer of it. Thus, the local gradient is the indicator of the changes that the weight parameters need to make and is an important reference for weight adjustment. In this paper, the local gradient on the $s-th$ neuron of the $i+1-th$ layer to $i-th$ layer is defined as:

$$\delta^i_s = f'\left(x^i_s\right) \sum\nolimits_j \delta^{i+1}_j w^{i+1}_{j,s} \tag{8}$$

where x^i_s is the input of the $s-th$ neuron of the $i-th$ layer, and $w^{i+1}_{j,s}$ is the weight between the $j-th$ neuron of the $i-1-th$ layer and the $s-th$ neuron of the $i-th$ layer. Therefore, we can train the neural network using the above momentum scheme.

V. DISCUSSION

In this section, the performance results of the prediction model are first presented. Then, we evaluate the performance of the prediction model and finally give a forward design method of standard driving posture based on the prediction model.

A. SIMULATION RESULTS

The performance of the DNN used in our design is presented in FIGURE 8. Obviously, we can obtain the prediction results quickly, even less than 50 epochs. Moreover, the training accuracy and prediction accuracy are as high as 97% and 88%, respectively, which shows that the test accuracy of the proposed prediction scheme meets the performance requirements and has good robustness.

FIGURE 9 shows the 3D surface of parameters related to driving posture. It is obvious that the 3D surface of the predicted driving posture almost matches that of the actual driving experience. Thus, it illustrates the feasibility of our designed driving posture prediction scheme.

B. PERFORMANCE EVALUATION

In addition, using the driving posture analysis module of RAMSIS [33], about 94 analysis models were built, as shown in FIGURE 10.

Comparing the model output results and the current design from the market, we can see that the convergence of the SgRP predicted by the model is better than the comparison data,

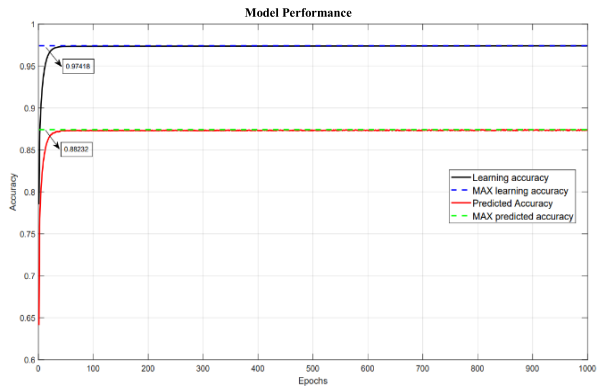

FIGURE 8. The performance of the DNN-based prediction model.

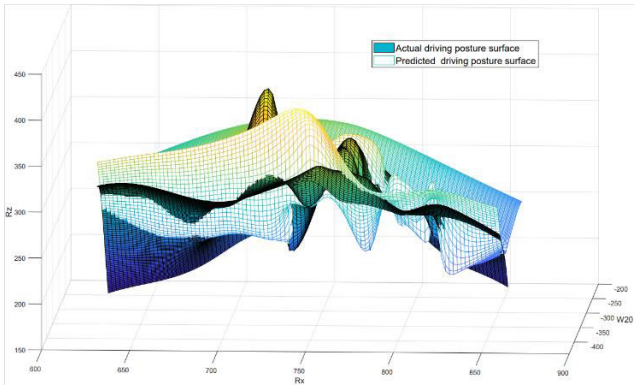

FIGURE 9. 3D surface of standard driving posture.

FIGURE 10. Driving posture analysis model of RAMSIS.

which means the robustness of the model is good, as shown in FIGURE 11.

C. FORWARD DESIGN OF DRIVING POSTURE

After defining the RgRP point, we need to set the seat travel box, which is the H point area. We used the intelligent

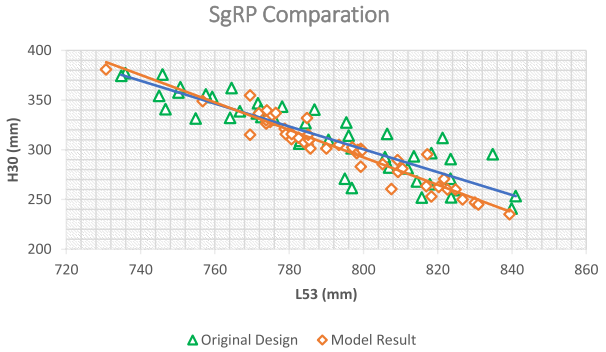

FIGURE 11. Comparison of RgRP.

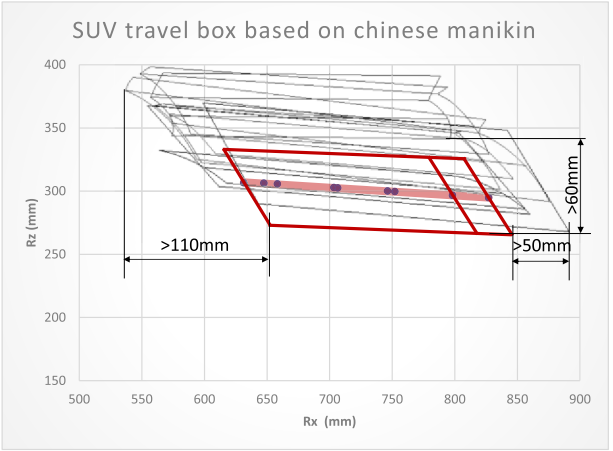

FIGURE 12. Comparison of the driver's travel box.

prediction model of this article to guide the forward design of a certain SUV based on the Chinese human body. The design results show that it is significantly different from the common cars of the same level in the market. The red area is the travel box based on the Chinese human body, and the gray ones are the actual travel box of the most sold market product of the same level. FIGURE 12 shows that the variations in standard driving posture among individuals are significant. Therefore, it is crucial to make personalized predictions based on the human body to provide better active and passive safety protection to the driver during the motion reconstruction of a vehicle takeover.

VI. LIMITATION

Due to the limitations of data acquisition conditions, experimental costs, model complexity, and point cloud processing methods, the sample size of the data set is small, which ultimately would affect the model's accuracy.

Besides, considering the research workload and the convenience of parameter selection, only the body height dimension was selected in the model input, while the body proportions and fatness were not considered, which would lead to bias in the personalized prediction of the model.

In future research, a new dataset would construct based on the current dataset to enrich the dimensionality of human parameters. The synthetic dataset would be considered and the real vehicle dataset as the supplement, so that to further expand the sample size of the dataset, which would further improve the accuracy of the algorithm model, and realize data-driven personalized standard driving posture prediction.

VII. CONCLUSION

In this study, a substantial number of vehicle driving posture parameters were obtained through laser scanning technology. A standard driving posture dataset was then constructed based on a weight analysis of the influencing factors. Utilizing this dataset, an intelligent standard driving posture prediction model was developed, laying a solid foundation for the reconstruction of non-standard driving postures.

REFERENCES

[1] V. Beanland, M. Fitzharris, K. L. Young, and M. G. Lenné, "Driver inattention and driver distraction in serious casualty crashes: Data from the Australian national crash in-depth study," *Accident Anal. Prevention*, vol. 54, pp. 99–107, May 2013.

[2] K. Lipovac, M. Derić, M. Tešić, Z. Andrić, and B. Marić, "Mobile phone use while driving-literary review," *Transp. Res. F, Traffic Psychol. Behaviour*, vol. 47, pp. 132–142, May 2017.

[3] M. Née, B. Contrand, L. Orriols, C. Gil-Jardiné, C. Galéra, and E. Lagarde, "Road safety and distraction, results from a responsibility case-control study among a sample of road users interviewed at the emergency room," *Accident Anal. Prevention*, vol. 122, pp. 19–24, Jan. 2019.

[4] S.-A. Kaye, S. Demmel, O. Oviedo-Trespalacios, W. Griffin, and I. Lewis, "Young drivers' takeover time in a conditional automated vehicle: The effects of hand-held mobile phone use and future intentions to use automated vehicles," *Transp. Res. F, Traffic Psychol. Behaviour*, vol. 78, pp. 16–29, Apr. 2021.

[5] B. W. Weaver and P. R. DeLucia, "A systematic review and meta-analysis of takeover performance during conditionally automated driving," *Human Factors, J. Human Factors Ergonom. Soc.*, vol. 64, no. 7, pp. 1227–1260, Nov. 2022.

[6] B. Zhang, J. de Winter, S. Varotto, R. Happee, and M. Martens, "Determinants of take-over time from automated driving: A meta-analysis of 129 studies," *Transp. Res. F, Traffic Psychol. Behaviour*, vol. 64, pp. 285–307, Jul. 2019.

[7] B. Thierry, M. Cunneen, M. Mullins, F. Murphy, F. Pütz, F. Spickermann, C. Braendle, and M. F. Baumann, "From semi to fully autonomous vehicles: New emerging risks and ethico-legal challenges for human-machine interactions," *Transp. Res. F, Traffic Psychol. Behav.*, vol. 63, p. 15364, 2019.

[8] *Driver Selected Seat Position*, Standard SAE-J1517, SAE, Warrendale, PA, USA, 1998.

[9] S. J. Park, C.-B. Kim, C. J. Kim, and J. W. Lee, "Comfortable driving postures for Koreans," *Int. J. Ind. Ergonom.*, vol. 26, no. 4, pp. 489–497, Oct. 2000.

[10] C. R. Mehta and V. K. Tewari, "Seating discomfort for tractor operators—A critical review," *Int. J. Ind. Ergonom.*, vol. 25, no. 6, pp. 661–674, Jul. 2000.

[11] C. Chunlei, *Research on Technology of Ergonomics Design Based on Driving Posture Prediction Model*. Hangzhou, China: Zhejiang University. 2005.

[12] M. Kolich, N. Seal, and S. Taboun, "Automobile seat comfort prediction: Statistical model vs. artificial neural network," *Appl. Ergonom.*, vol. 35, no. 3, pp. 84–275, 2004.

[13] S. Sun, "A support vector regression-based driver seat comfort evaluation method," *China Mech. Eng.*, vol. 19, no. 11, pp. 1326–1330, 2008.

[14] P. Wei, *Research on Vehicle Ride Comfort Evaluation Method*. Zhenjiang, China: Jiangsu University, 2017.

[15] J. Gou, "Machine learning based intelligent posture design of driver," *IOP Conf. Ser., Earth Environ. Sci.*, to be published.

[16] J. Gou, *Research on the Design Method of Driver'S Posture Based on Chinese Manikin*. Shanghai, China: Tongji University, 2017.

[17] C. Song, X. Bi, and J. Gou, "Design of reference points for driver's seat based on ergonomics comfort," in *Proc. Annu. Conf. China Soc. Automot. Eng.*, 2014, pp. 1464–1468.

[18] *Devices for Use in Defining and Measuring Vehicle Seating Accommodation*, Standard SAE J826, SAE, Warrendale, PA, USA, 2008.

[19] *Motor Vehicle Drivers'Eye Location*, Standard SAE J941, SAE, Warrendale, PA, USA, 2002.

[20] *Motor Vehicle Dimensions*, Standard SAE J1100, SAE Warrendale, PA, USA, 2009.

[21] *Accommodation Tool Reference Point*, Standard SAE J1516, SAE, Warrendale, PA, USA, 2011.

[22] J. Gou, J. Chuan, H. Wang, and Y. Gao, "Machine learning based intelligent posture design of driver," *J. Phys., Conf.*, vol. 1802, no. 3, Mar. 2021, Art. no. 032131.

[23] M. S. Mahmud, J. Z. Huang, S. Salloum, T. Z. Emara, and K. Sadatdiynov, "A survey of data partitioning and sampling methods to support big data analysis," *Big Data Mining Analytics*, vol. 3, no. 2, pp. 85–101, Jun. 2020.

[24] T. Yang and H. Xue, "Removal of scattered noise based on data of the cranial point cloud of the zokor head," in *Proc. Int. Conf. Comput. Inf. Big Data Appl. (CIBDA)*, Guiyang, China, Apr. 2020, pp. 75–78.

[25] V. Kumar and C. Khosla, "Data cleaning—A thorough analysis and survey on unstructured data," in *Proc. 8th Int. Conf. Cloud Comput., Data Sci. Eng. (Confluence)*, Noida, Jan. 2018, pp. 305–309.

[26] A. Kadadi, R. Agrawal, C. Nyamful, and R. Atiq, "Challenges of data integration and interoperability in big data," in *Proc. IEEE Int. Conf. Big Data (Big Data)*, Washington, DC, USA, Oct. 2014, pp. 38–40.

[27] L. Zhao, Z. Chen, Y. Hu, G. Min, and Z. Jiang, "Distributed feature selection for efficient economic big data analysis," *IEEE Trans. Big Data*, vol. 4, no. 2, pp. 164–176, Jun. 2018.

[28] Z. Huang, T. Xie, T. Zhu, J. Wang, and Q. Zhang, "Application-driven sensing data reconstruction and selection based on correlation mining and dynamic feedback," in *Proc. IEEE Int. Conf. Big Data (Big Data)*, Washington, DC, USA, Dec. 2016, pp. 1322–1327.

[29] M. Mito, K. Murata, D. Eguchi, Y. Mori, and M. Toyonaga, "A data reconstruction method for the big-data analysis," in *Proc. 9th Int. Conf. Awareness Sci. Technol. (iCAST)*, Fukuoka, Sep. 2018, pp. 319–323.

[30] J. Nie, J. Yan, H. Yin, L. Ren, and Q. Meng, "A multimodality fusion deep neural network and safety test strategy for intelligent vehicles," *IEEE Trans. Intell. Vehicles*, vol. 6, no. 2, pp. 310–322, Jun. 2021.

[31] E. A. Roxas, R. R. P. Vicerra, L. A. G. Lim, J. C. D. Cruz, R. Naguib, E. P. Dadios, and A. A. Bandala, "Multi-scale vehicle classification using different machine learning models," in *Proc. IEEE 10th Int. Conf. Humanoid, Nanotechnol., Inf. Technol., Commun. Control, Environ. Manage. (HNICEM)*, Baguio City, Philippines Nov. 2018, pp. 1–5.

[32] R. Zhang, P. Xie, C. Wang, G. Liu, and S. Wan, "Classifying transportation mode and speed from trajectory data via deep multi-scale learning," *Comput. Netw.*, vol. 162, Oct. 2019, Art. no. 106861.

[33] D. Hartmut, J. Speyer, C. Pruett, and H. Rothaug, "RAMSIS application guide step by step," Human Solutions GmbH, Kaiserslautern, Germany, Tech. Rep., 2005, pp. 3–28.

JUNJIE GOU (Member, IEEE) was born in Shanxi, China, in 1986. He received the B.S. degree in vehicle engineering from Shandong University, China, in 2009, and the M.S. degree in vehicle engineering from Tongji University, China, in 2017. He is currently pursuing the Ph.D. degree.

From 2009 to 2020, he was a senior engineer of the automobile company. His current research interests include ergonomics, vehicle platform architecture, and machine learning applications in driving posture research.

MINGMING ZHAO received the Ph.D. degree from Tongji University, Shanghai, China, in 2021. His current research interests include traffic accident in-depth investigation, vehicle active/passive safety systems development, image processing, artificial intelligence, human posture monitoring, and human movement analysis and simulation.

HONGYAN WANG is currently a Professor and a Doctoral Supervisor with Tongji University. In the past ten years, she has studied with the University of Stuttgart, Ford Motor Company, and Federal Highway Administration, Germany. She has participated in cooperation as a senior visiting scholar, for eight times. She has published ten monographs, including ''Automobile Structural Mechanics and Finite Element'' and published more than 60 articles in domestic and international journals. Her current research interests include the simulation calculation analysis of the safety of automobile body structure, the data analysis of traffic accidents, ergonomics, and automobile safety. Her research results won the Second Prize of Shanghai Science and Technology Progress, in 2002, and the Second Prize of Shanghai Automobile Industry Science and Technology Progress, in 2004.

XIAN WU is currently a Professor and a Doctoral Supervisor with Tongji University. He has published more than 25 articles in domestic and international journals and has applied for 23 patents. His current research interests include vehicle integration technology, lightweight automobile, and the control of vehicle noise. His research results won the Third Prize of Shanghai Science and Technology Progress, in 2009.